PCCP

Accepted Manuscript

ROYAL SOCIETY OF CHEMISTRY

www.rsc.org/pccp

PCCP: Physical Chemistry of Nanoparticles

Physicochemical characterization of nanoparticles and their behavior in the biological environment

L. Treuel[1,2,*], K. A. Eslahian[1], D. Docter[3], T. Lang[1], R. Zellner[2], K. Nienhaus[4], G. U. Nienhaus[4,5], R. H. Stauber[3] and M. Maskos[1]

(1) Fraunhofer ICT-IMM, Carl-Zeiss-Str. 18-20, 55129 Mainz, Germany
(2) Institute of Physical Chemistry, University of Duisburg-Essen, 45141 Essen, Germany
(3) Molecular and Cellular Oncology/Mainz Screening Center (MSC), University Hospital of Mainz, Langenbeckstr. 1, 55101 Mainz, Germany
(4) Institute of Applied Physics, Karlsruhe Institute of Technology (KIT), 76128 Karlsruhe, Germany
(5) Department of Physics, University of Illinois at Urbana-Champaign, Urbana, IL 61801, USA
*Correspondence should be addressed to: lennart.treuel@uni-due.de / lennart.treuel@imm.fraunhofer.de

Abstract

Whilst the physical and chemical properties of nanoparticles in the gas or idealized solvent phase can nowadays be characterized with sufficient accuracy, this is no longer the case for particles in the presence of a complex biological environment. Interactions between nanoparticles and biomolecules are highly complex on a molecular scale. The detailed characterization of nanoparticles under these conditions and the mechanistic knowledge of their molecular interactions with the biological world is, however, needed for any solid conclusions with regards to the relationship between the biological behavior of such particles and their physicochemical properties.

In the present article we discuss some of the problems with characterization and behavior of nanoparticles that are associated with their presence in chemically complex biological environments. Our focus is on the stability of colloids as well as on the formation and characteristics of protein coronae that have recently been shown to significantly modify the properties of pristine particles. Finally, we discuss the perspectives that may be expected from an improved understanding of nanoparticles in biological media.

1. Introduction

The detailed knowledge about physical and chemical aspects associated with the behavior of nanoparticles (NPs) in biological systems has now been recognized as a critically important in understanding nano-toxicology [1, 2] and in shaping the future of nano-medical [3, 4] applications.

Within the framework of the Priority Programme "Bio-Nano-Responses" (SPP1313) of the Deutsche Forschungsgemeinschaft (DFG) and beyond, the authors of this perspective article have been devoted to characterizing the physical and chemical properties of NPs that may affect their behavior in the biological world. While some of these aspects are of general importance to both *in vitro* and *in vivo* applications of NPs, others seem mainly relevant to *in vitro* conditions. Here, we critically review, the importance of physical and chemical NP properties, their thorough characterization and the implications to NP behavior in the biological world.

NPs are of similar size as many subcellular components and, therefore, may escape many of the established biological defense mechanisms directed against particulate matter. They typically highjack the endocytosis machinery to enter cells [4, 5]. Once inside the cells, they have been shown to cause adverse effects [6] and permanent cell damage [7, 8] including oxidative stress, inflammation, genetic damage, and the inhibition of cell division and cell death [9-12].

NPs from organic (e.g., viruses, coal, humic substances etc.) or inorganic (e.g., silicates, oxides, carbonates, metal sulfides etc.) material have always existed as part of the natural environment [13, 14]. Anthropogenically generated NPs with a further increased variance in composition, deliberate stabilizing features and other physical and chemical properties add to the complexity of biological responses. Moreover, particle concentrations in intended – or unintended – exposure scenarios may vary significantly from those for which biological defense mechanisms were established.

Nanomaterials may also dissolve in the biological milieu [15]. For example, metallic NPs release metal ions, which can have severe toxic effects [16]. Epple and co-workers [17] showed that the dissolution of Ag NPs leads to a steady-state ion concentration within a few hours. The degree and the kinetics of degradation were interpreted as a function of NP concentration, surface functionality and temperature [17]. Similar effects were reported for W-C/Co [18] NPs and Fe/Pt NPs [19] as well as for oxidic NPs like ZnO and CeO_2 [20]. It was also specifically pointed out that even NPs made from very low soluble substances such as SiO_2 degrade as function of

their size [21]. Such experimentally observed degradation rates of silica NPs were in good agreement with Gibbs free energy governed formation-dissolution mechanisms [22].

Low pH, which is realized in different compartments of a cell or an organism, may accelerate degradation. For example, NPs with a calcium phosphate precipitate core were observed to completely degrade within a few minutes at low pH within lysosomes [23]. This controlled process might allow these sponge-like NPs to be employed as efficient gene delivery vehicles [24].

Many physical and chemical interactions define the behavior of NPs in any biological environment. Here, NPs are exposed to relatively high physiological ion concentrations[25], pH changes[23] and a huge variety of biomolecules, predominantly proteins that may adsorb onto the NP surfaces[26-28]. All these interactions can strongly affect the colloidal stability of the NPs, alter or camouflage the particle surface, promote dissolution[17] and change the molecular-scale interaction with cells [4, 29]. An in-depth discussion of the basic physical interactions occurring at the nano-bio interface was presented by Nel and co-authors [30]. Here, we will discuss the direct effects of these interactions on the NPs and their individual properties as well as their consequences for *in vitro* studies involving NPs and for *in vivo* applications of such particles.

2. Stability of nanoparticles in chemically complex environments

2.1 Effect of the surrounding medium on NP stability

Engineered NPs are usually stabilized by electrostatic repulsion, steric hindrance, or depletion forces [31-33]. Steric stabilization is realized by macromolecules attached to the NP surface. An effective approach of two such stabilized colloids is impeded by thermodynamic forces [34] as a function of the polymer chain stiffness and the resulting entropic elasticity [35]. Charged functional groups or surfactant molecules on the NP surface produce a Coulomb potential and, thus, give rise to electrostatic repulsion between individual particles carrying charges of the same polarity. Such electrostatic stabilization can be qualitatively described by the Derjaguin-Landau-Verwey-Overbeek (DLVO) theory [36-38]. Short-ranged, attractive, van-der-Waals-type forces dominate at small inter-particle distances and give rise to the pronounced tendency of NPs to aggregate. Aggregation, however, is prevented by the longer-ranging Coulomb forces between charge-stabilized NPs. Both van-der-Waals-type and electrostatic forces are quantitatively affected by the ionic strength of the surrounding medium. Effective

van-der-Waals interactions between particles and the surrounding medium are expressed by the Hamaker constant, H [39]. As described by the Lifshitz theory [40], zero frequency contributions to dispersion forces, $H_{\nu=0}$, are lowered with increasing ionic strengths, whereas higher frequency terms, $H_{\nu>0}$, remain unaffected since the frequencies of oscillating dipoles are much higher than the time scales of ionic responses [41]. Accounting for these contributions, the effective Hamaker constant can be expressed by

$$H = H_{\nu=0} 2\kappa d \exp(-2\kappa d) + H_{\nu>0}, \qquad \text{(eq. 1)}$$

where d is the distance from the particle surface, and κ is the inverse Debye screening length, which describes the range of action of interacting electrostatic forces [42]:

$$\kappa = \sqrt{\frac{2F^2}{\varepsilon_0 \varepsilon_s RT} I}, \qquad \text{(eq. 2)}$$

with the Faraday constant, F, the permittivity of free space, ε_0, the relative permittivity of the solvent, ε_S, the universal gas constant, R, the absolute temperature, T, and the ionic strength of the solvent, I. In physiological media, the ionic strength is typically around 150 mM, yielding a highly compressed electrical double-layer and a Debye screening length κ^{-1} of 0.78 nm [25], which is smaller than the typical size of a protein (a few nanometers). Accordingly, the electrostatic stabilizing barrier is decreased significantly by increasing ionic strength (see Fig. 1).

Fig. 1a schematically illustrates the effect of the ionic strength on the interaction potential as a function of the distance from the NP surface. At physiological ion concentrations, charge-stabilized NPs frequently show a strong tendency to aggregate due to the decreased Coulomb repulsion at these conditions [43-45].

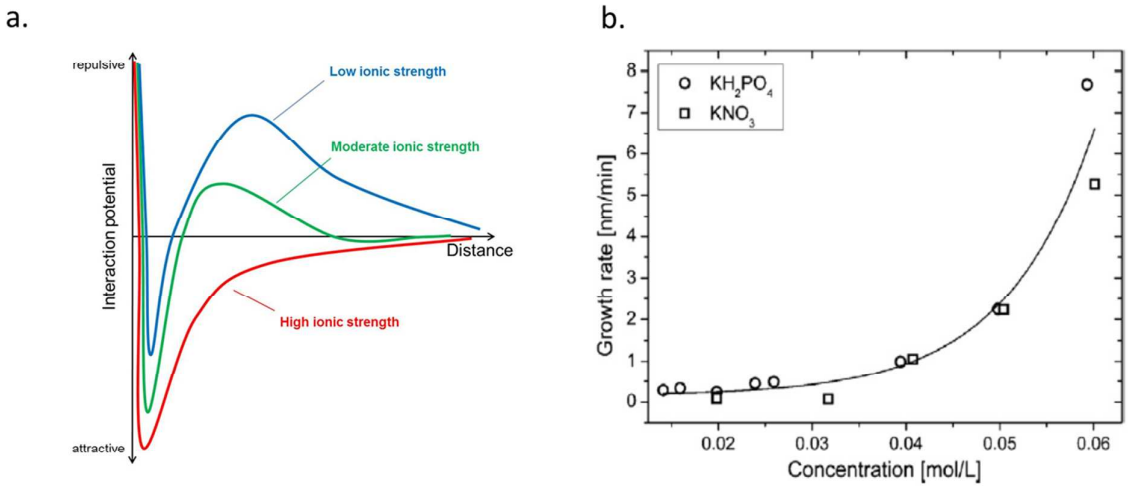

Fig. 1: (a) Impact of ionic strength on effective electrostatic forces as a function of the distance from the NP surface. In low ionic strength media, Coulomb interaction gives rise to strongly repulsive potentials. By moderately increasing the ionic strength, electrostatic forces are decreased but still produce a repulsive aggregation barrier, whereas a further increase of ionic strength (e.g., to the ionic strength of physiological buffer systems) leads to a concomitant decrease of the electrostatic forces. As a result, the stabilizing barrier is lost, and the overall net interaction is attractive, hence, particle aggregation takes place. (b) Growth rates (in nm/min) of a Lee-Meisel type silver colloid subjected to different concentrations of KH_2PO_4 and KNO_3 respectively. The observed growth is a consequence of NP aggregation following the destruction of the repulsive barrier [45]. Reprinted from Journal of Colloid and Interface Science, J.S. Gebauer, l. Treuel, Influence of individual ionic components on the agglomeration kinetics of silver nanoparticles, Pages 546–554, Copyright (2011), with permission from Elsevier [45].

Gebauer and Treuel [45] quantified the influence of individual ionic components on the aggregation kinetics of citrate stabilized silver NPs. They destabilized the NP suspension by adding defined amounts of salt and measured the increase in particle size that occurred as a consequence of agglomeration. Using this procedure, they determined growth rates of the particles as a function of KH_2PO_4 and KNO_3 concentrations respectively, demonstrating how both single-charged electrolytes have the same effect on the aggregation kinetics of the silver colloid (see Fig. 1b). Combining these results with Raman measurements of the water near-structure, they provide a further indication that ionic influences on the H-bonding network between water molecules rather than a direct interaction between ionic compounds and the particle surface affects agglomeration. Moreover, they demonstrated that this kinetic approach

could be used as a comparatively simple and yet potent method to measure average elementary charges on the colloidal NPs.

Considerable differences in the influence of equally charged but chemically different salts on the agglomeration behavior of colloids were found - commensurate with the Hofmeister-series[46] - that are largely ignored in the parameterizations of theoretical models describing agglomeration. This illustrates the complexity of NP stability even in such relatively simple environments where only the stabilized particles, water and defined amounts of chemically well-known ions are present. The plethora of molecular substances present in physiological fluids changes, and further complicates, this situation.

2.2 Role of the protein corona for NP stability

Besides the changes in ionic strength, physical and chemical interactions with proteins and other biomolecules (e.g., phospholipids, sugars, nucleic acids etc.) affect the NP behavior. Overall protein concentrations in typical body fluids (*e.g.*, blood, lung lining fluid, saliva, intestinal juice) can be as high as 0.35 g mL^{-1} [47], and such fluids may contain more than 3 000 different proteins in widely varying concentrations [48].

When NPs are exposed to body fluids, proteins rapidly bind to the NP surfaces and enshroud the particle [4, 27, 49-53]. This protein adsorption layer on the NP surface, the protein corona, largely defines the particle surface and mediates further interactions between the NP and the biological environment [47, 54]. Consequently, living organisms almost exclusively interact with protein-coated rather than as-synthesized NPs [4, 26, 47, 54], unless the NPs have been coated with a protein-repellant surface. The properties of such a protein-NP complex can differ significantly from those of the synthesized NP, and the nature of the protein corona is considered to be a potent factor in triggering desired and undesired biological responses [55-57].

Protein corona formation can affect both the NP and the adsorbed proteins in multiple ways. The protein structure can be impaired as a consequence of the interaction [4, 26, 58-61] which may lead to the loss of biological activity [62-64], exposure of cryptic epitopes [47, 65] or altered function [51, 52, 54]. The exact mechanistic details of such surface induced protein denaturation remain in the focus of current research and are not yet fully understood [30, 66-68].

Besides camouflaging the original NP surface, the protein corona can affect the colloidal stability of the NPs in the presence of physiological electrolyte concentrations [26, 51, 52, 54-56, 69], by steric or electro-steric effects. In a recent publication, Treuel and co-workers [60] were able to quantitatively demonstrate the stabilizing effect of a protein corona. They induced a constant agglomeration rate to a citrate (charge) stabilized suspension of Ag NPs by adding carefully controlled amounts of K_2SO_4 (this salt was chosen to avoid the possible precipitation of insoluble silver salts). This colloid was subjected to human serum albumin (HSA) at different concentrations, and the concentration dependence of the agglomeration rate was measured. Intriguingly, the protein concentration needed to fully stabilize the NPs directly corresponded to the amount of protein needed to fully cover the NP surface in a face-on configuration.

Introducing a new model based on statistical considerations of the collision geometries, Treuel *et al.* [60], could show that a plot of the surface coverage versus the logarithmic protein concentration allowed the evaluation of the data via a fitting routine using the Hill equation [70-73] (Fig. 2).

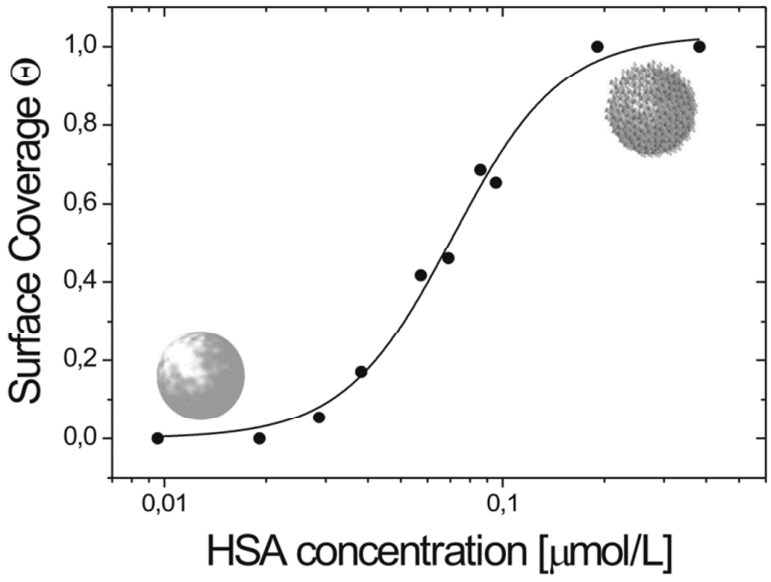

Fig. 2: Plot of experimental data of surface coverage versus the logarithmic HSA-concentration from a study of HSA adsorption onto citrate functionalized Ag NP surfaces. Surface coverage was inferred from the stabilizing effect of the HSA corona forming around a destabilized colloid. Black dots: data points, black solid line: Hill fit to the data points ($K_D = 71 \pm 17$ nmol·L^{-1}, n = 2.71) indicating a cooperative binding behavior. Reproduced with kind permission from Gebauer *et al.* [60]. Copyright 2012 American Chemical Society.

This quantitative evaluation revealed an equilibrium constant of $K_D = 71 \pm 17$ nmol·L^{-1}. The authors point out that K_D values for protein adsorption/desorption onto NP surfaces should generally be interpreted with caution as it remains unclear to what extent the interpretation as a true equilibrium situation is valid and what factors might limit this treatment. Possible factors determining limitations for an equilibrium treatment likely include NP properties such as surface chemistry, charge and size but also protein properties such as size, distribution of surface charge, stability, exposure of functional groups and others.

The affinity of a protein to a NP surface has been shown to depend on the NP surface coating [69, 74] and on the protein identity and function [75]. This effect has also been shown for *in vivo* conditions, where protein absorption onto injected polyethylene glycol (PEG) coated particles was found to be minimal, which led to longer circulation times and altered biodistribution [76]. However, the mechanistic details of these findings remain unclear and links between the full complexity of the *in vivo* situation and the *in vitro* experiments providing mechanistic information remain to be established further.

3. Detection and behavior of nanoparticles under biological conditions

3.1 Strengths and limitations of available detection techniques

NP size strongly determines the interaction with biological matter. It may even be modified due to adsorption of biomolecules and, hence, any size characterization should generally be performed in the same media employed in subsequent *in vitro* or *in vivo* applications [5]. Various experimental methods have been developed for size quantification under physiological conditions, having their specific advantages but also disadvantages. Under physiological conditions, the stability of colloids is often impaired so that, as time progresses, increasing amounts of aggregates may be formed. Particular methods may have different sensitivity toward the resulting, time-dependent variability in polydispersity. Combining different characterization methods can be a viable strategy to compensate drawbacks and remove the uncertainties of individual methods and, thus, provide a good trustworthy approximation of the actual size distribution [77].

Scanning electron microscopy (SEM) and transmission electron microscopy (TEM) are frequently applied to provide an overview on size and morphology of colloidal samples. However, for room temperature preparations, sample drying is required to achieve the necessary high vacuum. This process can produce severe artifacts in the obtained micrographs. Large numbers of particles need to be imaged and analyzed individually to

obtain sufficient statistics. High ion (and biomolecule) concentrations in physiological samples may generate significant background levels from which non-metal colloids can hardly be resolved. These disadvantages can be avoided by measurements at cryogenic temperatures with shock-frozen particles in solidified amorphous surrounding medium [78, 79].

NPs deposited on a flat substrate may also be visualized by atomic force microscopy (AFM), which is based on the force acting between the thin tip of a cantilever and the sample. As in electron microscopy, sample preparation for AFM can lead to substantial changes in physiological samples. With AFM experiments, force-distance curves (FD) can be measured to reveal the interaction forces. In combination with analytical ultra-centrifugation (AUC) and sodium dodecyl sulfate polyacrylamide gel electrophoresis (SDS-PAGE), FD curves have been measured to investigate interaction forces between SiO_2 and CeO_2 NPs and serum proteins. Significant differences between individual particle species were found, arising from small differences in their physicochemical properties [80]. FD curves in the liquid state have also been presented to observe particle-particle interactions in biological media. The aggregation behavior of CeO_2 particles in Roswell Park Memorial Institute (RPMI) medium was shown to be inversely dependent on the size of primary particles, whereas aggregation of Fe_2O_3 NPs in RPMI was claimed to be independent of particle size [81].

A popular method to measure size distributions of NPs under physiological conditions is dynamic light scattering (DLS). It involves the time-dependent measurement of the intensity of visible light scattered coherently by colloidal particles. Intensity fluctuations arise due to time-dependent variations of interfering contributions from particles diffusing randomly through the sample. The autocorrelation of the recorded intensity traces provides insight into the size and polydispersity of colloid samples. The scattering intensity is a function of the scattering angle; the angular distribution depends on the size and shape of the observed NPs. Because the scattered intensity scales with the particle radius to the sixth power, agglomerates, which may result from NP destabilization in biological environments, will dominate the scattered intensity. Moreover, all particles present in a biological sample, e.g., proteins, and other bio-matter, contribute to the scattered light and obscure the information about the colloidal NPs. This problem is exacerbated for organic NPs, which typically have a refractive index close to that of the surrounding bio-matter. As a result, the characterization of heterogeneous biological samples by DLS is very challenging, and multi-angle detection combined with experimental and theoretical expertise is required to obtain meaningful data [82,

[83]. In contrast, automated devices using simplified models based on spherical particles and Gaussian size distribution may not be able to resolve the properties in complex samples.

By time-averaged static light scattering (SLS), molecular weight averages of polymeric materials, averaged radii of gyration and second virial coefficients of NP interactions can be obtained as well. The ρ ratio, i.e., the quotient of hydrodynamic radius and radius of gyration, also includes information on the particle morphology [82].

Fluorescence correlation spectroscopy (FCS) involves the measurement of brief bursts of light emitted by single fluorophores as they diffuse through a small volume (typically 1 femtoliter) defined by a tightly focused laser beam [84]. Autocorrelation analysis of the fluorescence emission time traces yields a characteristic time scale of diffusion, τ_D, from which – as in DLS – the hydrodynamic radius, R_H, can be calculated with sub-nanometer precision by using the Stokes–Einstein equation. Therefore, FCS has been demonstrated to be an excellent technique for studying NP-protein interactions [44, 71, 85, 86]. A refined variant of the FCS method, dual-focus FCS (2fFCS), includes an absolute calibration standard and, therefore, promises to make high-precision particle size measurements even easier [87]. For example, 2fFCS has been used to determine the thickness of various protein coronae on FePt NPs with high precision so that the specific orientation of the adsorbed proteins on the NP surface could be inferred [75]. Unlike DLS, FCS requires particles that emit strong fluorescence, i.e., autofluorescent particles or particles labeled with fluorescent markers. However, this can also be advantageous because the measured signal arises solely from the fluorescent particles. Furthermore, the fluorescent particles need to be present in the sample at very low concentration, typically 1 nM. We note in addition that FCS is exquisitely sensitive to the presence of aggregates and thus can only be applied to samples with good colloidal stability.

Another valuable method to obtain size distributions of NPs is based on the tracking of Brownian motion of NPs by automated detection of their mean-squared displacement as a function of time. This information is related to the diffusion coefficient via the Einstein-Smoluchowski equations and the Stokes-Einstein relation [45, 59]. As confirmed by DLS, agglomeration of Ag NPs in RPMI medium was found to be affected by the presence of proteins using this technique [69]. Agglomeration occurred within a few hours in pure RPMI and RPMI-bovine serum albumin, whereas particles remained well-dispersed in RPMI-fetal calf serum.

Yet another approach to NP size analysis is analytical separation, as done in field-flow fractionation (FFF) [88]. In asymmetrical flow field-flow fractionation (AF-FFF), particles are displaced in a parabolic solvent flow by cross flow acting in rectangular direction. Elution time is a function of the diffusion coefficient and thus can be correlated to the hydrodynamic radius of particles [89, 90]. As a main feature for characterization of NPs in the biological environment, FFF is combined with other (detection) methods by online coupling, making use of the relatively monodisperse fractions eluting from the channel. Powerful characterization methods are online couplings of FFF with SLS [91], DLS [92], small-angle X-ray scattering (SAXS) [93], or inductively coupled plasma mass spectrometry (ICPMS) [94]. Also preparative fractionations have been realized by the circular asymmetrical flow field-flow eluator (CAFFFE) [95]. One main drawback of FFF in physiological salt conditions is dominating van der Waals-interaction between channel boundaries and NPs [96]. Direct display of the size distribution in FFF, allowed for quantification of size increase of superparamagnetic iron oxide NPs (SPIONs) in presence of plasma proteins [97].

3.2 Size determination of kinetically unstable colloids

At physiological salt concentrations, the stability and, hence, the time scale of colloidal aggregation can change drastically in the case of charge-stabilized NPs (Cho et al. 2008, Jiang et al. 2009a, Gebauer and Treuel 2011), leading to a steady formation of aggregates in the detection volume. Depending on the method used for size determination, this will affect the observations. In TEM and AFM, aggregates formed as a result of the drying process cannot be distinguished from aggregates that were already present in the original solution. In cryo-TEM, quantitative data evaluation of images is based on counting particle numbers. Thus, the probability of rarely formed aggregates to be detected in such an approach is rather small, especially at an early state of aggregation.

Methods such as DLS, which are based on coherent scattering, have a strong bias toward large and hence more strongly scattering particles. In fact, the presence of a few large aggregates can dominate the scattered intensity. Multi-component analysis of scattering intensities of NPs and proteins allow analysis of agglomerates by DLS [98]. However, this treatment neglects variations of the scattering intensity arising from increasing size of the primary NPs due to protein binding and, in addition, the possible changes in the size distribution of dissolved proteins that may change as a result of selective binding processes.

Where sedimentation of aggregated particles occurs, primary particles remain dispersed in the detection volume, whereas larger aggregates sediment at a much higher velocity, resulting in inadequate hydrodynamic radii to be obtained from DLS or Brownian motion analysis. In contrast, FFF can be applied to monitor agglomeration as di-, tri- or oligomers of primary particles will elute at larger retention times of the elugrams[99].

3.3 Effect of diffusion and sedimentation on dose rates in biological experiments

Exposure experiments of cells to NPs are most frequently performed in the presence of NP suspensions for which only the total mass concentration of the NPs is recorded, irrespective of the dispersity of the NPs. The net flux per time of the total NP mass to the cell surface, however, is in fact size selective due to a competition between diffusion and sedimentation.

Xia and co-workers[100] presented a detailed study elucidating the effect of sedimentation and diffusion on cellular uptake of gold NPs. In most *in vitro* experiments, the uptake of NPs is measured in a setup where cells reside at the bottom of a culture plate and are exposed to a supernatant suspension of NPs. As we have discussed above, many colloids are unstable under cell culture conditions, and agglomerates will form with significantly altered diffusion and sedimentation properties. Increased sedimentation, however, leads to a situation where the NP concentration on the cell surface can be markedly higher than the initial bulk concentration. This means that the factual dose rate to the cell membrane is not necessarily a simple function of the initial NP concentration but is significantly affected by NP stability.

In their study[100], Xia and co-workers quantified this problem by comparing cellular uptake of their NPs in the classical upright experimental configuration to the uptake in an inverted setup where the cultured cells were suspended from above with the cells facing the bottom of the well (see Fig. 3). Their study revealed strong differences in the cellular uptake dependent on the diffusion and sedimentation properties of the colloid and, hence, on the experimental setup.

This work strongly emphasizes the dire need for a thorough physical and chemical characterization of NPs under the experimental conditions of *in vivo* and *in vitro* experiments. Biological effects observed in such experimental approaches may frequently be artefacts of an ill-characterized colloidal stability. Here, the established methods and models of physics and physical chemistry can bring yet another strong contribution to the highly interdisciplinary field of nano-research.

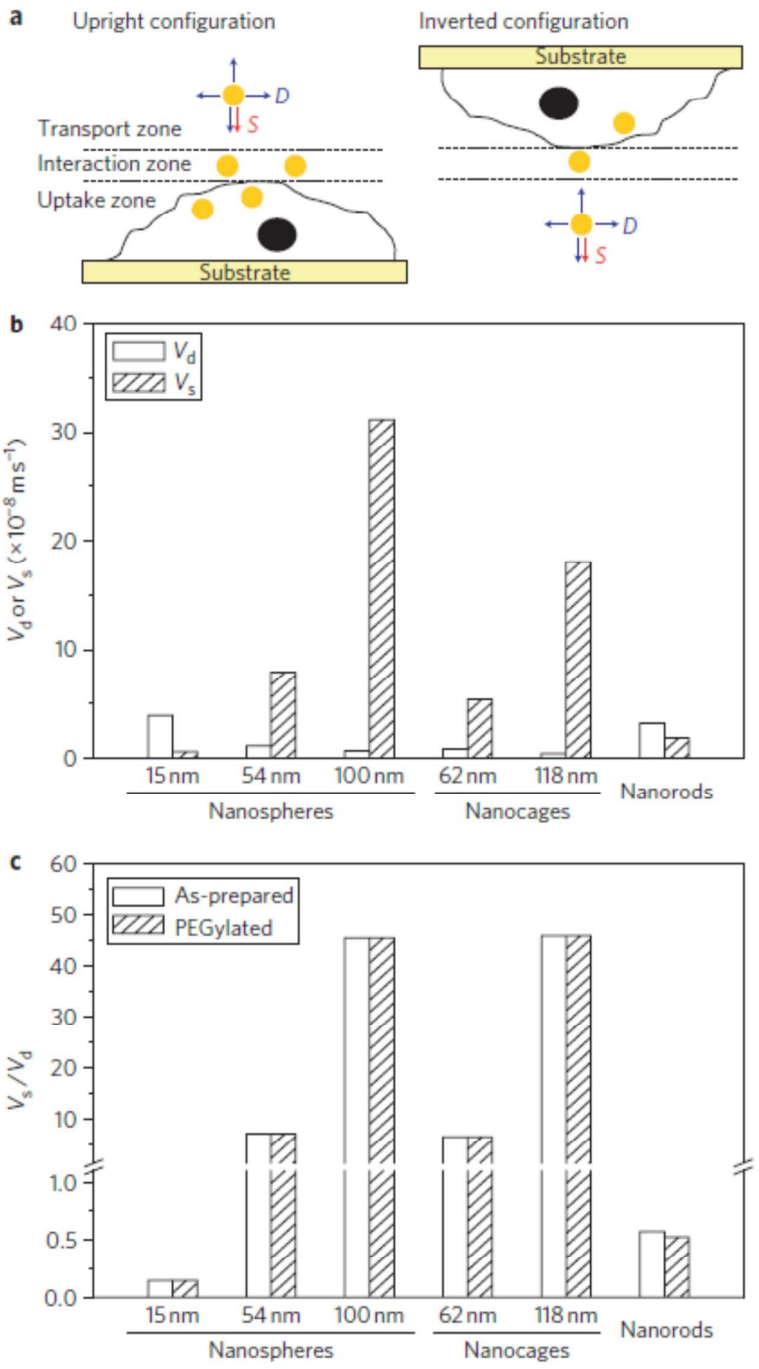

Fig. 3: (**a**) Schematic representation of the classic upright (left) and the inverted (right) cell culture setups used in the experiments to study the uptake of gold NPs. Transport, interaction and uptake zones are shown for both configurations. NP concentrations in the interaction zone of both concentrations depends on the sedimentation (S) and diffusion (D) characteristics of the NPs. (**b**) Quantification of the diffusion (V_d) and sedimentation (V_s) velocities of different types as-prepared NPs. (**c**) Ratios of sedimentation and diffusion velocities (V_s/V_d) for the different types of NPs used in the study. These ratios determine the dominant factor for NP transport to the cell surface and, hence, the factual dose rate. [100]

4. The protein corona

4.1 Fundamental aspects of corona formation

Many existing studies of the complex composition and time evolution of the protein corona are largely descriptive and go astray where detailed mechanistic explanation would be desirable [4, 26, 101]. Thermodynamic aspects of the interaction process between NPs and proteins are manifold including electrostatic, H-bonding and van-der-Waals type interactions, and lead to a complex situation. Detailed information about the NP surface is frequently not known on an atomic scale, and surface restructuring and ageing processes might occur during the interaction. Often times, this problem may be less severe considering that the protein is relatively large compared to a typical atomic binding site on the NP surface and, hence, its binding behavior will always be an average over a larger surface area.

An important role is played by ligands on the NP surface, that either results from the synthesis of the NPs themselves, or from consecutive synthetic chemistry. The potential exchange of ligands on the NP surface will strongly depend on the chemical type of the surface and on the bonding structure. Whilst some ligands can easily be exchanged in an equilibrium fashion, others, such as polymer coatings, were indicated to have a higher persistence on the NP surface, leading to a situation where they shield the underlying particle surface and mediate the interaction with proteins, rather than being exchanged.

A very critical aspect concerns the protein itself: The protein structure determines its solubility. Protein denaturation upon surface adsorption creates a situation where the desorbing, denatured protein molecule has an altered solubility compared to the native protein. This contradicts an equilibrium treatment since the adsorbing and desorbing species differ in their structure and properties. In addition, solvent effects need to be considered. The exact quantitative details of these processes remain to be uncovered [26].

Isothermal titration calorimetry (ITC) was suggested as a suitable method for studying the affinity and stoichiometry of protein binding by Cedervall, Linse, Dawson and co-workers [54], and others have adopted this approach[102]. In light of the complexity of the factual situation with many thermodynamic processes occurring simultaneously (*e.g.*, possible ligand exchange, possible changes in protein structure, changes in the solvation shells around protein and NP, *etc.*) the interpretation of such results requires great caution.

The first example of how protein adsorption can quantitatively follow a binding isotherm was presented by Nienhaus and co-workers [71], who analyzed the adsorption of human serum albumin (HSA) onto small (10–20 nm in diameter) polymer-coated, fluorescently labeled FePt and CdSe/ZnS NPs displaying carboxyl functions on the surface. With sub-nanometer precision, they measured the thickness of an HSA corona that formed around these NPs using fluorescence correlation spectroscopy (FCS). They showed that a protein layer of 3.3 nm thickness formed around their NPs, commensurate with a single protein layer (Fig. 4)

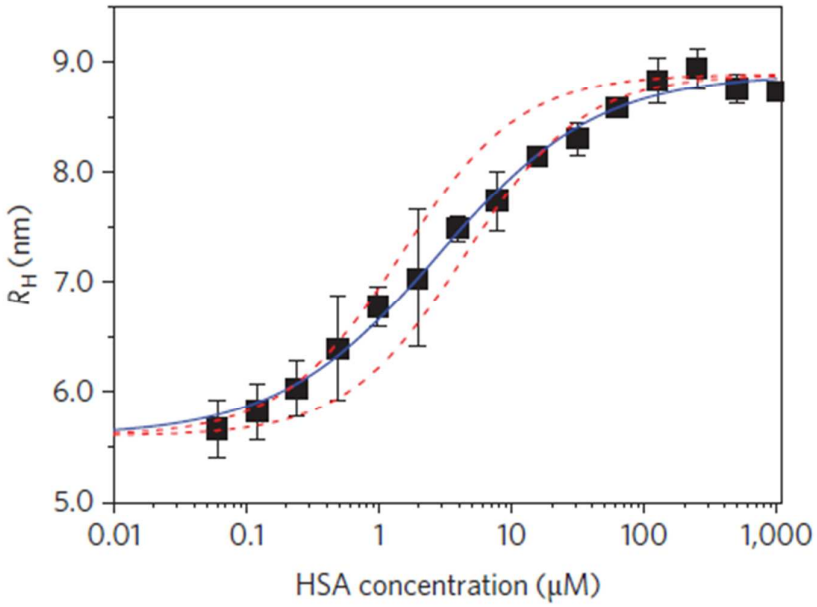

Figure 4: Binding curve illustrating the formation of an HSA corona on polymer-coated FePt NPs (measured by fluorescence correlation spectroscopy, FCS). The hydrodynamic radii of NPs are plotted as a function of HSA concentration with data-points being averages from three independent sets of measurements. The solid line (blue) represents a fit of an anti-cooperative Hill binding model to the data, and the dashed lines (red) are Langmuir binding isotherms fitted to the first and last 20% of the transition, illustrating the anti-cooperative behavior. (Reproduced with kind permission from Röcker et al. [71])

In a different study, also utilizing the FCS method, Milani et al. [85] studied the adsorption of transferrin onto sulfonate- and carboxyl-functionalized polystyrene NPs. They measured molar concentrations of fluorescently labeled proteins free in solution and bound to the NP surface. Adsorption curves resulting from their measurements indicate a universal behavior as a function of the protein/NP molar ratio, which was interpreted as a transition from monolayer coverage to multilayer adsorption. Moreover, they looked into the dynamics of the protein

adsorption layer and found different timescales, which they attributed to proteins bound in the first monolayer and to those being part of the secondary and ternary layers respectively. The first monolayer showed off-rates longer than the experimental time scale of a few hours, whilst the other shells appeared to exchange proteins on a time scale faster than minutes under buffer conditions. This same split-up in the off-rates was found for both surface functionalities used in their study but both off-rates were considerably faster in case carboxyl-functionalized NPs.

These results seem to be at variance with the results by Jiang et al. [103], who found monolayer formation for transferrin binding to carboxyl-functionalized, polymer-coated FePt NPs. In this work, the time dependence of the intensity autocorrelation function was analyzed to obtain the size of the NP/protein complex, which is a robust procedure yielding sub-nanometer size resolution (see also Fig. 4). Also, different NP surfaces, different relative nanoparticle-protein size ratios and indeed different proteins can all significantly alter the observed behavior [26, 59, 75, 104]. We shall discuss below how the interplay of different proteins can complicate this situation even further.

In a different study, the Nienhaus group gave a first indication of possible structure-activity relationships that might govern the protein corona formation [75]. Here, they pointed to the role of charged patches on the protein surface in shaping the adsorption orientation of corona proteins. This time using dual-focus fluorescence correlation spectroscopy (2fFCS), they indicated that both the binding affinities and the monolayer thicknesses, based on the known structural properties of the proteins, could be related to the presence of positively charged patches on the protein surface.

The claim that such patches, rather than the overall protein charge, govern the NP-protein interaction seems plausible, considering the sub-nanometer Debye shielding length under such conditions. As discussed above, the Debye length is considerably smaller than the average size of a protein, leading to a situation where no relevant Coulomb-type interactions occur between the NP and parts of an adsorbed protein that are not in close contact with the NP.

Treuel, Nienhaus and co-workers[105] have recently modified HSA, to alter its surface charge distribution and investigated the consequences for protein corona formation around small (radius ~5 nm), dihydrolipoic acid-coated quantum dots (DHLA-QDs) by using fluorescence correlation spectroscopy. Not only did these charge modifications alter the corona thickness indicating distinctly different protein orientations on the NP but also the affinity was strongly

affected. Notably, their work convincingly demonstrated the reversibility of protein binding for their NP/protein systems, independent of the modification[105]. They were also able to show the effect of the differently modified coronae on the extent and kinetics of internalization of their NPs by HeLa cells. From these experiments, they revealed pronounced variations in the cellular uptake that indicate how even small physicochemical changes of the protein corona may significantly affect biological responses[105].

This rare example of a structure-affinity relation that was reported in this work emphasizes once more the importance of very basic physico-chemical experiments to elucidate the factual situation. Such data remain scarce, but many experimental techniques are readily available for studying the structure of proteins in solution and in NP-protein aggregates, including but not limited to circular dichroism [26, 59, 104, 106-108], Fourier transform infrared spectroscopy [109-111], Raman spectroscopy / SERS [104, 112, 113] and fluorescence spectroscopy [71, 75, 85, 114, 115], size-exclusion chromatography (SEC) [116-121], isothermal titration calorimetry (ITC) [102, 122] and surface plasmon resonance (SPR) [54, 123].

Many additional factors may affect the protein corona, such as variations in temperature or pH. Lesniak, Dawson and co-workers studied the serum corona formation around polystyrene NPs, revealing significant differences in the cellular uptake if their NPs were incubated in heat inactivated serum compared to not heat inactivated serum [124]. Further addressing the molecular aspects of these findings, Mahmoudi et al. concluded from their experiments that changes in the incubation temperature can cause severe differences in protein corona formation, degree of surface coverage and composition, although, as they point out, this may not necessarily always be the case [125]. The exact physiological implications of these findings remain somewhat vague, since rarely temperature varies as a sole factor in a biological system. The same holds true for changes in pH: They are frequently associated with a preceding membrane transfer and it is not yet established what happens to the corona during such membrane penetration processes [4, 111].

4.2 Simulations of nanoparticle-protein interactions by computational modelling

To resolve molecular mechanisms of corona formation, computational modelling can provide a valuable tool in bridging the gap between experimental findings and the underlying molecular information [126].

Dell'Orco, Linse and co-workers modelled the competing adsorption of three different proteins (human serum albumin, high density lipoprotein and fibrinogen) onto 70 nm copolymer (N-iso-propylacrylamide/N-tert-butylacrylamide) NPs based on individual affinities, rate constants and stoichiometry in human blood [127]. Recently, Darbai Sahneh *et al*. expanded this approach by nonlinear dynamics techniques, describing the dynamics of corona formation from population balance equations [128]. Their model predicts a rapid formation of a protein corona with a metastable composition, determined by association rates and weighted by corresponding initial protein concentrations. As continuous association and dissociation of proteins to the NP surface continues, their model predicts a stable corona composition, determined by the product of equilibrium constants and the initial individual protein concentrations. Intriguingly, this prediction is very well in line with experimental findings of a corona hardening at longer timescales [26, 54, 129-131] and is a god example of how relatively simple model approaches can help to describe specific aspects of the factual situation even under very complex chemical and biological conditions. Such models may also help to improve the design of experimental approaches and their combination with further methods of computational simulation may provide a valuable tool for a molecular understanding of experimental observations.

While molecular dynamics (MD) approaches were shown to describe the molecular systems of proteins and NPs rather well [132-137], the large system size and the relatively long timescales of corona formation complicate the modelling of this process [138-140]. Multi-level approaches and coarse-grained simulations have therefore been adopted to studying corona formation processes [101, 132, 136, 139], however, still with a rather limited predictive power for the physiological situation or chemically/biologically complex systems [139, 141-144]. Despite these current problems, such atomistic level in silico approaches can be a useful tool to complement experimental studies of NP-protein interactions and reveal some of the molecular scale driving forces for the experimentally observed situation[145-149].

Wang and co-workers used a combined experimental and model approach to understand the adsorption of bovine serum albumin (BSA) onto CTAB (cetyltrimethylammonium bromide)-coated Au nanorods (aspect ratio: 4.2, mean length: 56 nm)[136]. Using synchrotron radiation

for X-ray near-edge structure (XANES)[150], they investigated binding of sulfur (from cysteine residues) to the Au surface. In their corresponding MD simulations, Wang *et al.* [136] initially placed one BSA molecule next to the Au surface and applied a driving force of 100 pN on the sulfur atoms for binding of cysteine groups. They found reduction of 6 disulfide bonds and continuous binding of 12 cysteine groups on the surface within a small time scale of 140 ns. It should be noted, that is an extremely rapid process, compared to typical experimental observation times under physiological conditions. The ongoing conformational change was shown to change even after successful binding to form an extended contact area. It contributed to an unfolding of alpha helical structure which has also been shown before on similar surfaces by circular dichroism [26, 59, 104] and SERS spectroscopy [104, 151].

Recently, Brancolini and co-workers used a combination of simulation methods at different levels of theory (including Brownian dynamics, classical atomistic MD and quantum mechanical DFT calculations) to study the adsorption of ubiquitin onto gold NPs [135]. Ubiquitin is a protein that is ubiquitously found in eukaryotes and does not contain cysteine residues (*i.e.*, no disulfide bonds or SH residues). Results of calculations presented in their manuscript advise a set of different structures for possible ubiquitin-gold complexes. They compared their results to experimental data (circular dichroism and NMR) and from this comparison, suggested that short-range, non-electrostatic interactions and binding to citrate were important parameters, in forming complexes most similar to the experimental results. Using the freedom of the theoretical approach, they also varied the surface conditions (bare, citrate covered), finding a situation where some citrate molecules were replaced by the adsorbing protein while other citrate molecules stayed attached to the surface, coexisting with the adsorbed ubiquitin molecules. While this is an interesting finding, the relevance in a more complex situation, such as physiological conditions, with many different proteins and other molecules of various sizes competing for binding to the NP surface, remains elusive. Also, under physiological conditions the strong interactions that become possible between cysteine residues of other proteins and the gold surface may be much more dominant than the effects described here. However, this work is an example of how experimental and theoretical techniques may be used in a complementing fashion, revealing information that cannot be inferred from one approach alone.

Another approach, combining experimental and multiscale molecular dynamics simulations, was presented by Ding et al., who studied the interaction between ubiquitin and the surfaces of silver NPs [139]. Their results revealed a competition of ubiquitin molecules and citrate for

binding to the NP surface, with ubiquitin replacing the surface bound citrate molecules. Intriguingly, their modeling results showed specific binding orientations between ubiquitin molecules and AgNP surfaces, driven by electrostatic interactions (Fig. 5). The importance of such electrostatic interactions for binding orientations and was lately demonstrated experimentally by Treuel et al.[105].

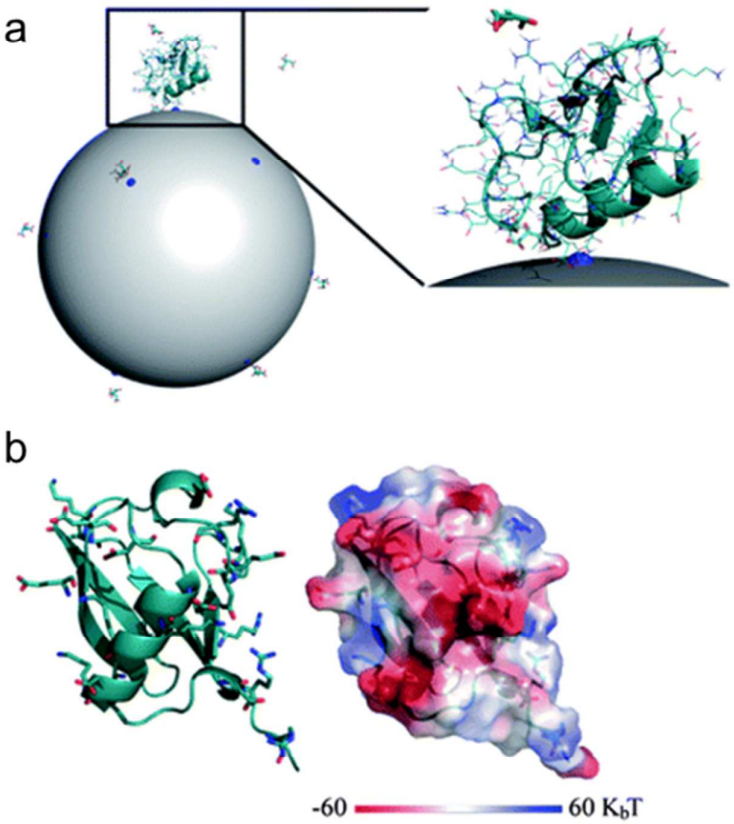

Fig. 5: Model results for the interaction between a single ubiquitin molecule and a citrate-coated AgNP. (a) Structure of the ubiquitin-AgNP complex in presence of citrate after t = 50 ns (ubiquitin is represented as backbone and ribbons with the side chains as lines and the citrate molecules as sticks. Gray sphere: Ag NP, charged atoms on the NP surface shown as blue spheres). The zoomed view of the final structure illustrates the binding between the ubiquitin molecule and a charged atom on the NP surface. (b): Left panel: Model representation of the ubiquitin molecule with the negatively (aspartate and glutamate) and positively (lysine and arginine) charged residues shown as red and blue sticks, respectively. Right panel: Surface electrostatic potential of the ubiquitin molecule, computed using PyMol (http://www.pymol.org). Figure adapted from Ding *et al.*, [135] with permission from the PCCP Owner Societies.

From both, their simulations and experiments, Ding and co-workers[139] concluded a loss of α-helical structure upon adsorption of ubiquitin onto the silver surfaces, which is well in line with earlier findings [59-61, 104, 151]. Further, their coarse-grained simulations of ubiquitin corona formation around their AgNPs, uncovered a stretched exponential binding kinetics that was found to be in good agreement with earlier reported experimental results [71].

This work is another example how MD simulations using simplified systems can indeed assist in understanding the molecular behavior governing the factual situation even under more complex experimental conditions. Yet, it is currently not clear to what extent the truly influential parameters governing the processes under physiologically relevant conditions have been truly identified in these simulation approaches.

4.3 Complexity of the protein corona under biological conditions

The formation of a protein layer on flat surfaces was first analyzed by Vroman in 1962 [152]. The corresponding "Vroman-effect" describes a time-dependent composition of the bio-coating, where the early state is dominated by highly abundant proteins, which adsorb only weakly. Subsequently, adsorbed proteins are replaced by less abundant proteins, which bind with greater affinity, resulting in a complex series of adsorption and displacement steps. By describing the concept of a "dynamic protein corona", the Vroman model was directly transferred to explain the evolution of the protein corona around NPs [130, 131]. In this model, the composition of the corona is predominantly controlled by the association and dissociation constant of various proteins. To fully understand the interaction of NPs with biological systems a time-resolved knowledge of NP-specific protein adsorption is required, as certain protein groups display increased or reduced binding over time. In this context, it was recently shown by Tenzer, Stauber and co-workers [28] for silica and polystyrene NPs of various sizes and surface-functionalization that the formation of a protein corona is a very rapid process. However, novel binding kinetics for biologically relevant protein groups have been discovered, which cannot be solely explained by the Vroman-effect. Classification of protein-binding modalities identified proteins characterized by low abundance at the beginning of plasma exposure and at later time points, but displaying "peak" abundance at intermediate time points and vice versa (Fig. 6).

Previous kinetic studies did not employ quantitative LC-MS-based proteomics, and these complex binding kinetics went unnoticed so far. In their study, Tenzer et al. [28] showed that the

binding patterns observed in the human blood plasma model cannot be explained by the current mathematical protein-corona-evolution models in simplified systems [60, 127, 131].

In the same study, the authors could show that the protein coronae formed very rapidly and exhibited an unexpected complexity on all investigated nanoparticles. Previous studies suggested that the protein corona consists of only a few tens of proteins, even when nanomaterials are introduced into a highly complex environment such as the human blood plasma [50, 56]. Tenzer et al. were able to detect and quantify as much as 166 different plasma corona proteins at the earliest exposure time point on all investigated nanoparticles. By extending their analyses to prolonged plasma exposure time points and by employing a latest generation label-free quantitative liquid chromatography mass spectrometry (LC-MS) instrument, they detected almost 300 different corona proteins for all exposure time points. Over the different investigated time-points the corona composition changed only quantitatively and not qualitatively.

The composition of the long-lived, so-called "hard" protein corona is clearly affected by NP properties, including size / surface curvature and zeta potential [27], surface functionalities [52], hydrophobicity [56] and topology [153]. But also the plasma exposure time was identified as an additional critical factor of nanoparticle-bound protein abundance. However, none of the above-mentioned factors (physicochemical properties of the NP and exposure time) alone is exclusively able to control formation, composition and evolution of the protein corona. A multi-parameter classifier will most probably be required to generally model and predict nanoparticle-protein interaction profiles in biological relevant environments [28, 50].

In the study by Tenzer et al. [28], the authors were able to show the (patho)biological relevance of the protein corona in *in vitro* studies of primary human cell models of the blood system. Pristine nanoparticles existed only for a short period of time, but could immediately affect vitality of endothelial cells, trigger thrombocyte activation and aggregation, and result in hemolysis. Formation of the biomolecule corona rapidly modulated the nanoparticles' decoration with bioactive proteins, thus, protecting cells of the blood system against nanoparticle-induced (patho)biological processes, and could also promote cellular uptake [28].

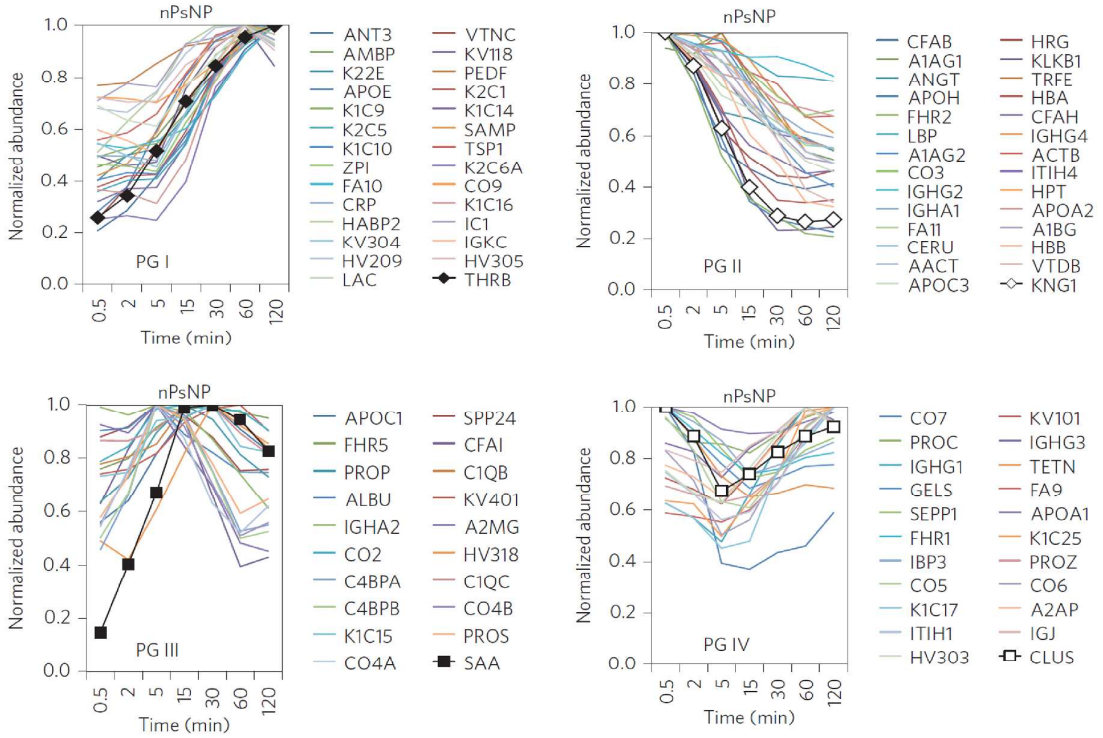

Fig. 6: Correlation analysis by Tenzer et al. [28] revealed distinct kinetic protein-binding modalities during corona evolution. Time-smoothed normalized protein abundance profile of nPsNPs (Polystyrene) nanoparticle coronas was classified into four groups by correlation analysis. Relative values normalized to the maximum amount (set to 1) across all time points for each protein. Protein groups PG I and PG II displayed increasing or reduced binding over time, respectively, and thus in a "Vroman-dependent manner". 'Peak' proteins (PG III) are characterized by low abundance at the beginning of plasma exposure and at later time points, but displaying peak abundance at intermediate time points. Other proteins (PG IV) show exactly the opposite behaviour, being highly abundant at early and late time points, but not at intermediate time points, "Vroman-independent manner". (Adapted with kind permission from Tenzer et al., [28])

5. Diagnostics employing NPs – an outlook

Owing to their special properties, the use of NPs in biomedical applications has been discussed for a long time [154-157], with the mainly desired goals of increasing therapeutic transport and efficacy and of minimizing toxic side effects [158].

While problems regarding the biological transport and safety of NPs persist, their successful application for *in vivo* diagnostic purposes has been shown [159-162]. NP-based diagnostic agents can improve the results of many existing readout techniques, including but not limited to fluorescence detection [163-167], magnetic resonance imaging (MRI) [168-172] and Radionucleide-

based imaging (*e.g.* SPECT, PET) [173-175]. Moreover, completely novel techniques become accessible for *in vivo* application by the use of NPs. For example, Nie and coworkers successfully demonstrated how surface enhanced Raman spectroscopy (SERS) labelled Au NPs could be used for tumor detection in live animals [162]. Their PEGylated SERS NPs were considerably brighter than semiconductor quantum dots and had a light emission in the near-infrared (NIR) window [162].

NPs can also be utilized to combine diagnostic and therapeutic properties in the same particle for so called „theranostic“ approaches [159, 160]. Such applications continue to receive much attention and will undoubtedly benefit from an improving molecular understanding of NP transport and behavior in biological systems.

Besides these *in vivo* uses, *in vitro* diagnostics can make good use of specific binding and imaging properties of NPs [176]. Sample preparation strategies have been developed to perform *in vitro* diagnostics in lab-on-a-chip applications [177, 178], enabling large numbers of accurate and precise measurements to be performed rapidly and by low costs.

In general, three basic strategies can be distinguished, in which NPs might be used for *in vitro* diagnostics: to mark, to sort and to encapsulate. Quantum dots and Au NPs are the most relevant species as markers and already industrially used in pregnancy tests or drug screening tests [179, 180]. Their main advantage compared to fluorescence marked sensors is the absence of bleaching phenomena. To enhance marking efficiency by gold NPs, synthesis of nanorods can drastically reduce the plasmon damping [181] and lead to an intensity increase, enabling single particle mapping [182]. Strategies for the use of nanocapsules are widely spread and include immobilization [183], transport [184, 185], or enhancement of bioactivities [186]. Besides, by encapsulation, liposomes can be used as nano-reactors of monodisperses Pd NPs [187].

In terms of imaging by specific sorting, magnetic NPs are proposed for purification and enrichment of nucleic acids and proteins [188]. Also, protein-conjugated magnetic beads were used for effective DNA-aptamer bindings on food allergens [189]. Immunomagnetic capture of cells was modeled in computational fluid dynamics (CFD) and sorting of circulating tumor cells was demonstrated using magnetic NPs [190]. Biomarker detection in blood plasma has also been shown by a one-step magnetic NP immunoassay [191]. Another example for magnetic sorting is provided for microfluidic DNA purification by centrifugation [192] and microfluidic allergy indication [193].

6. Conclusions and outlook

Despite the substantial developments of the past years, difficulties persist to link the physical and chemical properties of NPs to their biological effects. The complex chemical composition of the biological environment results in a multitude of competing effects and the relative timescales of these individual effects may be of significant importance.

Changes in colloidal stability are amongst the straightforward things that occur at the ambient ion concentrations of a biological fluid. While current models parameterize many of these ionic influences, they fall short of including effects that arise as consequences of biomolecule adsorption as discussed above [60]. We have discussed the stabilizing effect of the protein corona in case of charge stabilized silver NPs[60] and it should be noted in this context that *in vitro* uptake experiments are frequently carried out with higher NP concentrations than those expected for any environmental exposure of cells, even including intended exposure scenarios. The lower NP collision rates at relevant *in vivo* concentrations could well lead to situations where a destabilized colloid does not necessarily form agglomerates because it can be decorated and stabilized by proteins before relevant collisions between particles occur.

At common *in vitro* NP concentrations, agglomeration of NPs in cell culture medium is a formidable challenge for any quantitative evaluation of biological experiments involving NPs. Where dose rates become a function of NP stability and collision-rate (particle concentration) rather than original particle concentration, any underlying biological information is obscured by this effect. This becomes even more important since the cellular uptake of larger agglomerates may involve completely different endocytic pathways than the uptake of individual NPs and both may involve different time scales [44, 111].

The reliable determination of physical and chemical parameters of NPs in biological fluids remains a challenging task. We have discussed different techniques that are commonly employed in size characterization of NP suspensions and the difficulties that are introduced by the presence of a biological medium. Currently, reliable characterization data can only be obtained by employing multiple, complementing methods. We emphasize the urgent need that such characterization is carried out at the same conditions and the same timescales as the biological experiment. This is frequently not the case and this source of error presents a critical problem for any model developments or regulatory decision making.

Large gaps still exist in the understanding of the fundamental physicochemical aspects of corona formation and even larger gaps exist in applying this knowledge to a realistic

biological situation. Despite the discussed progress that has been made, the consequences of the protein corona and, hence, its properties on the biological behavior of NPs are still elusive and still poorly understood [1, 4, 130, 194, 195].

We have discussed the latest developments of Tenzer, Stauber and co-workers[28] showing that our current models of competitive adsorption fall short of explaining the factual physiological situation where NPs are subjected to thousands of different proteins competing for binding to their surface. Interestingly, the number of different proteins found to be bound to the NPs in their study exceeds the number of proteins that could be accommodated on a single NP, giving first indications for a statistical variance between the coronae of individual NPs in the same medium. This, and the fact that pure equilibrium treatments may not suffice to fully explain the factual situation, needs and deserves further attention.

Overall, the detailed kinetics of corona formation, stability and aging effects need further consideration. The development of the protein corona under complex biological conditions, with proteins exchanging with a multitude of competing proteins, is still only poorly understood and we stress the need to bridge the gap between the *in vitro* results, acquired under highly controlled conditions, and the *in vivo* consequences, which are still elusive [1, 26, 130, 194, 195].

Increased understanding will also lead to new rational designs of nanoparticle systems as well as new applications, e.g. design of multifunctional NPs will lead to increased sensitivities and possibilities for biomedical sensing [196-198]. On the other side, microfluidic lab-on-a-chip systems will help to monitor the cellular response to NPs exposure to avoid or replace otherwise necessary *in vivo* tests [199].

Acknowledgement

L. Treuel, R. Zellner, G. U. Nienhaus, R. H. Stauber and M. Maskos thank the Deutsche Forschungsgemeinschaft (DFG) for supporting this work within the Priority Programme "Bio-Nano-Responses" (SPP1313). LT acknowledges support by the Young Scientists Grant of the UDE and by the Bruno-Werdelmann Foundation.

7. References

1. G. Oberdörster, *J. Intern. Med.*, 2010, **267**, 89-105.
2. G. Oberdörster, *Environ. Health Perspect.*, 2012, **120**, A13.
3. P. Aggarwal, J. B. Hall, C. B. McLeland, M. A. Dobrovolskaia and S. E. McNeil, *Adv. Drug Deliv. Rev.*, 2009, **61**, 428-437.
4. L. Treuel, X. Jiang and G. U. Nienhaus, *J. R. Soc. Interface*, 2013, **10**, 20120939.
5. J. Kasper, M. I. Hermanns, C. Bantz, O. Koshkina, T. Lang, M. Maskos, C. Pohl, R. E. Unger and C. J. Kirkpatrick, *Arch. Toxicol.*, 2013, **87**, 1053-1065.
6. A. Manke, L. Wang and Y. Rojanasakul, *BioMed Res. Int.*, 2013, **2013**, 1-15.
7. P. V. Asha Rani, G. Low Kah Mun, M. P. Hande and S. Valiyaveettil, *ACS Nano*, 2008, **3**, 279-290.
8. O. Lunov, T. Syrovets, C. Röcker, K. Tron, G. U. Nienhaus, V. Rasche, V. Mailänder, K. Landfester and T. Simmet, *Biomaterials*, 2010, **31**, 9015-9022.
9. Y. Ju-Nam and J. R. Lead, *Sci. Total Environ.*, 2008, **400**, 396-414.
10. N. Li, T. Xia and A. E. Nel, *Free Radical Biology and Medicine*, 2008, **44**, 1689-1699.
11. V. Stone, H. Johnston and M. J. D. Clift, *IEEE Trans. Nanobiosci.*, 2007, **6**, 331-340.
12. H. J. Johnston, G. Hutchison, F. M. Christensen, S. Peters, S. Hankin and V. Stone, *Crit. Rev. Toxicol.*, 2010, **40**, 328-346.
13. P. Biswas and C. Y. Wu, *J. Air. Waste. Manag. Assoc.*, 2005, **55**, 708-746.
14. R. Owen and M. Depledge, *Mar. Pollut. Bull.*, 2005, **50**, 609-612.
15. S. K. Misra, A. Dybowska, D. Berhanu, S. N. Luoma and E. Valsami-Jones, *Sci. Total Environ.*, 2012, **438**, 225-232.
16. J. C. Wataha, C. T. Hanks and R. G. Craig, *J. Biomed. Mater. Res.*, 1993, **27**, 227-232.
17. S. Kittler, C. Greulich, J. Diendorf, M. Köller and M. Epple, *Chem. Mater.*, 2010, **22**, 4548-4554.
18. D. Kühnel, W. Busch, T. Meißner, A. Springer, A. Potthoff, V. Richter, M. Gelinsky, S. Scholz and K. Schirmer, *Aquat. Toxicol.*, 2009, **93**, 91-99.
19. C. Xu, Z. Yuan, N. Kohler, J. Kim, M. A. Chung and S. Sun, *J. Am. Chem. Soc.*, 2009, **131**, 15346-15351.
20. T. Xia, M. Kovochich, M. Liong, L. Mädler, B. Gilbert, H. Shi, J. I. Yeh, J. I. Zink and A. E. Nel, *ACS Nano*, 2008, **2**, 2121-2134.
21. T. Diedrich, A. Dybowska, J. Schott, E. Valsami-Jones and E. H. Oelkers, *Environ. Sci. Technol.*, 2012, **46**, 4909-4915.
22. W. Vogelsberger, *J. Phys. Chem. B*, 2003, **107**, 9669-9676.
23. J. Li, Y.-C. Chen, Y.-C. Tseng, S. Mozumdar and L. Huang, *J. Control. Release*, 2010, **142**, 416-421.
24. S. Bisht, G. Bhakta, S. Mitra and A. Maitra, *Int. J. Pharmaceut.*, 2005, **288**, 157-168.
25. B. W. Ninham and V. A. Parsegian, *J. Theor. Biol.*, 1971, **31**, 405-428.
26. L. Treuel and G. U. Nienhaus, *Biophys. Rev.*, 2012, **4**, 137-147.
27. S. Tenzer, D. Docter, S. Rosfa, A. Wlodarski, J. Kuharev, A. Rekik, S. K. Knauer, C. Bantz, T. Nawroth, C. Bier, J. Sirirattanapan, W. Mann, L. Treuel, R. Zellner, M. Maskos, H. Schild and R. H. Stauber, *ACS Nano*, 2011, **5**, 7155-7167.
28. S. Tenzer, D. Docter, J. Kuharev, A. Musyanovych, V. Fetz, R. Hecht, F. Schlenk, D. Fischer, K. Kiouptsi, C. Reinhardt, K. Landfester, H. Schild, M. Maskos, S. K. Knauer and R. H. Stauber, *Nat. Nanotechnol.*, 2013, **8**, 772-781.
29. X. Jiang, C. Röcker, M. Hafner, S. Brandholt, R. M. Dörlich and G. U. Nienhaus, *ACS Nano*, 2010, **4**, 6787-6797.
30. A. E. Nel, L. Mädler, D. Velegol, T. Xia, E. M. Hoek, P. Somasundaran, F. Klaessig, V. Castranova and M. Thompson, *Nat. Mater.*, 2009, **8**, 543-557.
31. D. H. Napper, *J. Colloid. Interface Sci.*, 1977, **58**, 390-407.
32. T. Tadros, in *Electrical Phenomena at Interfaces and Biointerfaces*, John Wiley & Sons, Inc2012, pp. 153-172.
33. R. I. Feigin and D. H. Napper, *J. Colloid. Interface Sci.*, 1980, **75**, 525-541.
34. K. Chen and Y. Ma, *J. Phys. Chem.*, 2005, **109**, 17617-17622.

35. J. D. Moroz and P. Nelson, *Macromolecules*, 1998, **31**, 6333-6347.
36. B. W. Derjagin and L. D. Landau, in *Acta. Physiochim. USSR.*, 14 edn., 1941, pp. 633-662.
37. E. J. W. Verwey and J. T. G. Overbeek, *Theory of the stability of lyophobic colloids*, Elsevier, Amsterdam, 1948.
38. J. N. Israelachvili, *Intermolecular and Surface Forces*, Elsevier professional, s.l, 2010.
39. H. C. Hamaker, *Physica*, 1937, **4**, 1058-1072.
40. L. D. Landau, E. M. Lifshitz and L. P. Pitaevskij, *Electrodynamics of continuous media*, Butterworth-Heinemann, Oxford, 1998.
41. W. Russel, D. Saville and W. Schowalter, *Colloidal Dispersions*, Cambridge University Press, Cambridge, 1989.
42. J. Lyklema, *Fundamentals of Interface and Colloid Science: Solid-Liquid Interfaces*, Elsevier professional, s.l, 1995.
43. K. Cho, Y. Lee, C.-H. Lee, K. Lee, Y. Kim, H. Choi, P.-D. Ryu, S. Y. Lee and S.-W. Joo, *J. Phys. Chem. C.*, 2008, **112**, 8629-8633.
44. J. Jiang, G. Oberdörster and P. Biswas, *J. Nanopart. Res.*, 2009, **11**, 77-89.
45. J. S. Gebauer and L. Treuel, *J. Colloid. Interface Sci.*, 2011, **354**, 546-554.
46. W. Kunz, *Curr. Opin. Colloid. Interface. Sci.*, 2010, **15**, 34-39.
47. J. Klein, *Proc. Natl. Acad. Sci. USA*, 2007, **104**, 2029-2030.
48. S. K. Jeong, M. S. Kwon, E. Y. Lee, H. J. Lee, S. Y. Cho, H. Kim, J. S. Yoo, G. S. Omenn, R. Aebersold, S. Hanash and Y. K. Paik, *Proteomics*, 2009, **9**, 3729-3740.
49. S. H. De Paoli Lacerda, J. J. Park, C. Meuse, D. Pristinski, M. L. Becker, A. Karim and J. F. Douglas, *ACS Nano*, 2010, **4**, 365-379.
50. A. Lesniak, F. Fenaroli, M. P. Monopoli, C. Åberg, K. A. Dawson and A. Salvati, *ACS Nano*, 2012, **6**, 5845-5857.
51. T. Cedervall, I. Lynch, M. Foy, T. Berggård, S. C. Donnelly, G. Cagney, S. Linse and K. A. Dawson, *Angew. Chem. Int. Ed.*, 2007, **46**, 5754-5756.
52. M. Lundqvist, J. Stigler, G. Elia, I. Lynch, T. Cedervall and K. A. Dawson, *Proc. Natl. Acad. Sci. USA*, 2008, **105**, 14265-14270.
53. I. Lynch, *Physica A.*, 2007, **373**, 511-520.
54. T. Cedervall, I. Lynch, S. Lindman, T. Berggård, E. Thulin, H. Nilsson, K. A. Dawson and S. Linse, *Proc. Natl. Acad. Sci. USA*, 2007, **104**, 2050-2055.
55. M. P. Monopoli, F. Baldelli-Bombelli and K. A. Dawson, *Nat. Nanotechnol.*, 2011, **6**, 11-12.
56. M. P. Monopoli, D. Walczyk, A. Campbell, G. Elia, I. Lynch, F. B. Bombelli and K. A. Dawson, *J. Am. Chem. Soc.*, 2011, **133**, 2525-2534.
57. I. Lynch, A. Salvati and K. A. Dawson, *Nat. Nanotechnol.*, 2009, **4**, 546-547.
58. S. Laera, G. Ceccone, F. Rossi, D. Gilliland, R. Hussain, G. Siligardi and L. Calzolai, *Nano Lett.*, 2011, **11**, 4480-4484.
59. L. Treuel, M. Malissek, J. S. Gebauer and R. Zellner, *Chem. Phys. Chem.*, 2010, **11**, 3093-3099.
60. J. S. Gebauer, M. Malissek, S. Simon, S. K. Knauer, M. Maskos, R. H. Stauber, W. Peukert and L. Treuel, *Langmuir*, 2012, **28**, 9673-9679.
61. L. Treuel and M. Malissek, in *Cellular and Subcellular Nanotechnology - Methods and Protocols*, eds. V. Weissig, T. Elbayoumi and M. Olsen, Springer Science+Business Media, New York, USA2013, pp. 225-235.
62. A. A. Vertegel, R. W. Siegel and J. S. Dordic, *Langmuir*, 2004, **20**, 6800-6807.
63. C. E. Rodriguez, J. M. Fukuto, K. Taguchi, J. Froines and A. K. Cho, *Chem. Biol. Interact.*, 2005, **155**, 97-110.
64. Z. J. Deng, M. Liang, M. Monteiro, I. Toth and R. F. Minchin, *Nat. Nanotechnol.*, 2011, **6**, 39-44.
65. I. Lynch, K. A. Dawson and S. Linse, *Science STKE*, 2006, **2006**, 14.
66. A. des Rieux, V. Fievez, M. Garinot, Y.-J. Schneider and V. Préat, *J. Control. Release*, 2006, **116**, 1-27.
67. M. Yan, J. Du, Z. Gu, M. Liang, Y. Hu, W. Zhang, S. Priceman, L. Wu, Z. Hong Zhou, H. Liu, T. Segura, Y. Tang and Y. Lu, *Nat. Nanotchnol.*, 2009, **5**, 48-53.
68. L. Liu, K. Xu, H. Wang, J. Tan P. K., W. Fan, S. S. Venkatraman, L. Li and Y.-Y. Yang, *Nat. Nanotechnol.*, 2009, **4**, 457-463.

69. S. Kittler, C. Greulich, J. S. Gebauer, J. Diendorf, L. Treuel, L. Ruiz, J. M. Gonzalez-Calbet, M. Vallet-Regi, R. Zellner, M. Köller and M. Epple, *J. Mater. Chem.*, 2010, **20**, 512-518.
70. E. L. Gelamo, C. H. T. P. Silva, H. Imasato and M. Tabak, *BBA - Protein Struct. M.*, 2002, **1594**, 84-99.
71. C. Röcker, M. Pötzl, F. Zhang, W. J. Parak and G. U. Nienhaus, *Nat. Nanotechnol.*, 2009, **4**, 577-580.
72. S. Goutelle, M. Maurin, F. Rougier, X. Barbaut, L. Bourguignon, M. Ducher and P. Maire, *Fundam. Clin. Pharmacol.*, 2008, **22**, 633-648.
73. A. V. Hill, *J. Physiol.*, 1910, **40**, 4-7.
74. R. H. Müller and C. M. Keck, *J. Nanosci. Nanotechnol.*, 2004, **4**, 471-483.
75. P. Maffre, K. Nienhaus, F. Amin, W. J. Parak and G. U. Nienhaus, *Beilstein J. Nanotechnol.*, 2011, **2**, 374-383.
76. D. E. Owens and N. A. Peppas, *Int. J. Pharmaceut.*, 2006, **307**, 93-102.
77. R. F. Domingos, M. A. Baalousha, Y. Ju-Nam, M. M. Reid, N. Tufenkji, J. R. Lead, G. G. Leppard and K. J. Wilkinson, *Environ. Sci. Technol.*, 2009, **43**, 7277-7284.
78. M. Adrian, J. Dubochet, J. Lepault and A. W. McDowall, *Nature*, 1984, **308**, 32-36.
79. W. Mueller, K. Koynov, K. Fischer, S. Hartmann, S. Pierrat, T. Basché and M. Maskos, *Macromolecules*, 2009, **42**, 357-361.
80. J. Schaefer, C. Schulze, E. E. J. Marxer, U. F. Schaefer, W. Wohlleben, U. Bakowsky and C.-M. Lehr, *ACS Nano*, 2012, **6**, 4603-4614.
81. G. Pyrgiotakis, C. O. Blattmann, S. Pratsinis and P. Demokritou, *Langmuir*, 2013, **29**, 11385-11395.
82. W. Schärtl, *Light Scattering from Polymer Solutions and Nanoparticle Dispersions*, Springer-Verlag, s.l, 2007.
83. M. Maskos and R. H. Stauber, in *Comprehensive Biomaterials*, ed. P. Ducheyne, Elsevier, Oxford2011, pp. 329-339.
84. L. Zemanová, A. Schenk, M. J. Valler, G. U. Nienhaus and R. Heilker, *Drug Discov. Today*, 2003, **8**, 1085-1093.
85. S. Milani, F. Baldelli Bombelli, A. S. Pitek, K. A. Dawson and J. Rädler, *ACS Nano*, 2012, **6**, 2532-2541.
86. G. U. Nienhaus, P. Maffre and K. Nienhaus, in *Methods Enzymol.*, ed. S. Y. Tetin, Academic Press2013, vol. 519, pp. 115-137.
87. T. Dertinger, V. Pacheco, I. v. d. Hocht, R. Hartmann, I. Gregor and J. Enderlein, *Chem. Phys. Chem.*, 2007, **8**, 433-443.
88. J. Giddings, *Science*, 1993, **260**, 1456-1465.
89. J. C. Giddings, *J. Chem. Educ.*, 1973, **50**, 667.
90. K. G. Wahlund and J. C. Giddings, *Anal. Chem.*, 1987, **59**, 1332-1339.
91. B. Wittgren, K.-G. Wahlund, M. Andersson and C. Arfvidsson, *Int. J. Polym. Anal. Charact.*, 2002, **7**, 19-40.
92. J. Ehrhart, A.-F. Mingotaud and F. Violleau, *J. Chromatogr. A.*, 2011, **1218**, 4249-4256.
93. P. Knappe, L. Boehmert, R. Bienert, S. Karmutzki, B. Niemann, A. Lampen and A. F. Thünemann, *J. Chromatogr. A.*, 2011, **1218**, 4160-4166.
94. B. Schmidt, K. Loeschner, N. Hadrup, A. Mortensen, J. J. Sloth, C. Bender Koch and E. H. Larsen, *Anal. Chem.*, 2011, **83**, 2461-2468.
95. M. Maskos and W. Schupp, *Anal. Chem.*, 2003, **75**, 6105-6108.
96. T. Lang, K. A. Eslahian and M. Maskos, *Macromol. Chem. Phys.*, 2012, **213**, 2353-2361.
97. J. Ashby, S. Schachermeyer, S. Pan and W. Zhong, *Anal. Chem.*, 2013, **85**, 7494-7501.
98. K. Rausch, A. Reuter, K. Fischer and M. Schmidt, *Biomacromolecules*, 2010, **11**, 2836-2839.
99. A. Roda, M. Mirasoli, D. Melucci and P. Reschiglian, *Clin. Chem.*, 2005, **51**, 1993-1995.
100. E. C. Cho, Q. Zhang and Y. Xia, *Nat. Nanotechnol.*, 2011, **6**, 385-391.
101. M. Mahmoudi, I. Lynch, M. R. Ejtehadi, M. P. Monopoli, F. B. Bombelli and S. Laurent, *Chem. Rev.*, 2011, **111**, 5610-5637.
102. G. Baier, C. Costa, A. Zeller, D. Baumann, C. Sayer, P. H. H. Araujo, V. Mailänder, A. Musyanovych and K. Landfester, *Macromol. Biosci.*, 2011, **11**, 628-638.
103. X. Jiang, S. Weise, M. Hafner, C. Röcker, F. Zhang, W. J. Parak and G. U. Nienhaus, *J. R. Soc. Interface*, 2010, **7**, S5-S13.

104. L. Treuel, M. Malissek, S. Grass, J. Diendorf, D. Mahl, W. Meyer-Zaika and M. Epple, *J. Nanopart. Res.*, 2012, **14**, 1102-1014.
105. L. Treuel, S. Brandholt, P. Maffre, S. Wiegele, L. Shang and G. U. Nienhaus, *ACS Nano*, 2014, doi:10.1021/nn405019v.
106. L. Shang, Y. Wang, J. Jiang and S. Dong, *Langmuir*, 2007, **23**, 2714-2721.
107. N. J. Greenfield, *Trends Anal. Chem.*, 1999, **18**, 236-244.
108. S. M. Kelly, T. J. Jess and N. C. Price, *Biochim. Biophys. Acta*, 2005, **1751**, 119-139.
109. K. K. Chittur, *Biomaterials*, 1998, **19**, 357-369.
110. J. Zhang and Y. B. Yan, *Anal. Biochem.*, 2005, **340**, 89-98.
111. T. Wang, J. Bai, X. Jiang and G. U. Nienhaus, *ACS Nano*, 2012, **6**, 1251-1259.
112. S. Schlücker, *Biophotonik*, 2008, **3**, 18-20.
113. M. Shao, L. Lu, H. Wang, S. Luo and D. Duo Duo Ma, *Microchim. Acta*, 2009, **164**, 157-160.
114. C. A. Royer, *Chem. Rev.*, 2006, **106**, 1769-1784.
115. L. Mátyus, J. Szöllösi and A. Jenei, *J. Photochem. Photobiol. B: Biol.*, 2006, **83**, 223-236.
116. M. Printz and W. Friess, *J. Pharmaceut. Sci.*, 2012, **101**, 826-837.
117. S. Mori and H. G. Barth, *Size exclusion chromatography*, Springer, Berlin, 1999.
118. J. F. Carpenter, T. W. Randolph, W. Jiskoot, D. J. A. Crommelin, C. R. Middaugh and G. Winter, *J. Pharmaceut. Sci.*, 2010, **99**, 2200-2208.
119. A. Vogt, C. D´Angelo, F. Oswald, A. Denzel, C. H. Mazel, M. V. Matz, S. Ivanchenko, G. U. Nienhaus and J. Wiedenmann, *PLoS ONE*, 2008, **3**, 1-8.
120. J. Wiedenmann, S. Ivanchenko, F. Oswald and G. U. Nienhaus, *Mar. Biotechnol.*, 2004, **6**, 270-277.
121. J. Wiedenmann, A. Schenk, C. Röcker, A. Girod, K. D. Spindler and G. U. Nienhaus, *Proc. Natl. Acad. Sci. USA*, 2002, **99**, 11646-11651.
122. G. U. Nienhaus, ed. *Protein-ligand interactions: methods and applications*, Humana Press, New York, 2005.
123. Y. Cheng, M. Wang, G. Borghs and H. Chen, *Langmuir*, 2011, **27**, 7884-7891.
124. A. Lesniak, A. Campbell, M. P. Monopoli, I. Lynch, A. Salvati and K. A. Dawson, *Biomater.*, 2010, **31**, 9511-9518.
125. M. Mahmoudi, A. M. Abdelmonem, S. Behzadi, J. H. Clement, S. Dutz, M. R. Ejtehadi, R. Hartmann, K. Kantner, U. Linne, P. Maffre, S. Metzler, M. K. Moghadam, C. Pfeiffer, M. Rezaei, P. Ruiz-Lozano, V. Serpooshan, M. A. Shokrgozar, G. U. Nienhaus and W. J. Parak, *ACS Nano*, 2013, **7**, 6555-6562.
126. A. S. Barnard, *Nat. Nanotechnol.*, 2009, **4**, 332-335.
127. D. Dell'Orco, M. Lundqvist, C. Oslakovic, T. Cedervall and S. Linse, *PLoS ONE*, 2010, **5**, e10949.
128. F. Darabi Sahneh, C. Scoglio and J. Riviere, *PLoS ONE*, 2013, **8**, e64690 EP.
129. M. P. Monopoli, D. Walczyk, A. Campbell, G. Elia, I. Lynch, F. Baldelli Bombelli and K. A. Dawson, *J. Am. Chem. Soc.*, 2011, **133**, 2525-2534.
130. E. Casals, T. Pfaller, A. Duschl, G. J. Oostingh and V. Puntes, *ACS Nano*, 2010, **4**, 3623-3632.
131. M. Lundqvist, J. Stigler, T. Cedervall, T. Berggård, M. B. Flanagan, I. Lynch, G. Elia and K. Dawson, *ACS Nano*, 2011, **5**, 7503-7509.
132. C. Ge, J. Du, L. Zhao, L. Wang, Y. Liu, D. Li, Y. Yang, R. Zhou, Y. Zhao, Z. Chai and C. Chen, *Proc. Natl. Acad. Sci. USA*, 2011, **108**, 16968-16973.
133. J. Shang, T. A. Ratnikova, S. Anttalainen, E. Salonen, P. C. Ke and H. T. Knap, *Nanotechnol.*, 2009, **20**, 415101.
134. T. A. Ratnikova, P. Nedumpully Govindan, E. Salonen and P. C. Ke, *ACS Nano*, 2011, **5**, 6306-6314.
135. G. Brancolini, D. B. Kokh, L. Calzolai, R. C. Wade and S. Corni, *ACS Nano*, 2012, **6**, 9863-9878.
136. L. Wang, J. Li, J. Pan, X. Jiang, Y. Ji, Y. Li, Y. Qu, Y. Zhao, X. Wu and C. Chen, *J. Am. Chem. Soc.*, 2013, **135**, 17359-17368.
137. G. Zuo, Q. Huang, G. Wei, R. Zhou and H. Fang, *ACS Nano*, 2010, **4**, 7508-7514.
138. F. Liu, X.-s. Ye, T. Wu, C.-T. Wang, J.-w. Shen and Y. Kang, *Sensors*, 2008, **8**, 8453-8462.
139. F. Ding, S. Radic, R. Chen, P. Chen, N. K. Geitner, J. M. Brown and P. C. Ke, *Nanoscale*, 2013, **5**, 9162-9169.

140. K. Kubiak and P. A. Mulheran, *J. Phys. Chem. B*, 2009, **113**, 12189-12200.
141. A. J. Makarucha, N. Todorova and I. Yarovsky, *Eur. Biophys. J.*, 2011, **40**, 103-115.
142. C.-c. Chiu, G. R. Dieckmann and S. O. Nielsen, *J. Phys. Chem. B*, 2008, **112**, 16326-16333.
143. C.-c. Chiu, G. R. Dieckmann and S. O. Nielsen, *Pept. Sci.*, 2009, **92**, 156-163.
144. A. Hung, S. Mwenifumbo, M. Mager, J. J. Kuna, F. Stellacci, I. Yarovsky and M. M. Stevens, *J. Am. Chem. Soc.*, 2011, **133**, 1438-1450.
145. J. J. Gray, *Curr. Opin. Struct. Biol.*, 2004, **14**, 110-115.
146. R. A. Latour, *Biointerphases*, 2008, **3**, FC2-FC12.
147. M. M. Harding, M. W. Nowicki, M. D. Walkinshaw, M. M. Harding, M. W. Nowicki and M. D. Walkinshaw, *Crystallogr. Rev.*, 2010, **16**, 247-302.
148. O. Cohavi, S. Corni, F. De Rienzo, R. Di Felice, K. E. Gottschalk, M. Hoefling, D. Kokh, E. Molinari, G. Schreiber, A. Vaskevich and R. C. Wade, *J. Mol. Recognition*, 2010, **23**, 259-262.
149. R. Di Felice and S. Corni, *J. Phys. Chem. Lett.*, 2011, **2**, 1510-1519.
150. J. Stöhr, *NEXAFS spectroscopy*, Springer, Berlin, 2003.
151. S. Grass and L. Treuel, *J. Nanopart. Res.*, 2014, **16**, 1-11.
152. L. Vroman, *Nature*, 1962, **196**, 476-477.
153. M. Mahmoudi, M. A. Shokrgozar, S. Sardari, M. K. Moghadam, H. Vali, S. Laurent and P. Stroeve, *Nanoscale*, 2011, **3**, 1127-1138.
154. T. M. Allen and P. R. Cullis, *Science*, 2004, **303**, 1818-1822.
155. D. G. Georganopoulou, L. Chang, J.-M. Nam, C. S. Thaxton, E. J. Mufson, W. L. Klein and C. A. Mirkin, *Proc. Natl. Acad. Sci. USA*, 2005, **102**, 2273-2276.
156. S. Gunawardena, *Pharmaceut. Res.*, 2013, **30**, 2459-2474.
157. G. L. Prasad, in *Safety of nanoparticles - from manufacturing to medical applications*, ed. T. J. Webster, Springer Science+Business Media, LLC, New York, USA2009, ch. 5.
158. J. R. Heath and M. E. Davis, *Annu. Rev. Med.*, 2008, **59**, 251-265.
159. J. Xie, S. Lee and X. Chen, *Adv. Drug. Del. Rev.*, 2010, **62**, 1064-1079.
160. S. M. Janib, A. S. Moses and J. A. MacKay, *Adv. Drug. Del. Rev.*, 2010, **62**, 1052-1063.
161. G. Bao, S. Mitragotri and S. Tong, *Annu. Rev. Biomed. Eng.*, 2013, **15**, 253-282.
162. X. Qian, X.-H. Peng, D. O. Ansari, Q. Yin-Goen, G. Z. Chen, D. M. Shin, L. Yang, A. N. Young, M. D. Wang and S. Nie, *Nat. Biotechnol.*, 2008, **26**, 83-90.
163. S. Kim, Y. T. Lim, E. G. Soltesz, A. M. De Grand, J. Lee, A. Nakayama, J. A. Parker, T. Mihaljevic, R. G. Laurence, D. M. Dor, L. H. Cohn, M. G. Bawendi and J. V. Frangioni, *Nat. Biotechnol.*, 2004, **22**, 93-97.
164. Y. Du, B. Xu, T. Fu, M. Cai, F. Li, Y. Zhang and Q. Wang, *J. Am. Chem. Soc.*, 2010, **132**, 1470-1471.
165. G. Hong, J. T. Robinson, Y. Zhang, S. Diao, A. L. Antaris, Q. Wang and H. Dai, *Angew. Chem. Int. Ed.*, 2012, **51**, 9818-9821.
166. E. Cassette, M. Helle, L. Bezdetnaya, F. Marchal, B. Dubertret and T. Pons, *Adv. Drug. Del. Rev.*, 2013, **65**, 719-731.
167. X. Wu, F. Tian, W. Wang, J. Chen, M. Wu and J. X. Zhao, *J. Mater. Chem. C*, 2013, **1**, 4676-4684.
168. O. T. Bruns, H. Ittrich, K. Peldschus, M. G. Kaul, U. I. Tromsdorf, J. Lauterwasser, M. S. Nikolic, B. Mollwitz, M. Merkel, N. C. Bigall, S. Sapra, R. Reimer, H. Hohenberg, H. Weller, A. Eychmuller, G. Adam, U. Beisiegel and J. Heeren, *Nat. Nanotechnol.*, 2009, **4**, 193-201.
169. K. Fan, C. Cao, Y. Pan, D. Lu, D. Yang, J. Feng, L. Song, M. Liang and X. Yan, *Nat. Nanotechnol.*, 2012, **7**, 459-464.
170. D. Ghosh, Y. Lee, S. Thomas, A. G. Kohli, D. S. Yun, A. M. Belcher and K. A. Kelly, *Nat. Nanotechnol.*, 2012, **7**, 677-682.
171. H. B. Na, I. C. Song and T. Hyeon, *Adv. Mater.*, 2009, **21**, 2133-2148.
172. D. Yoo, J.-H. Lee, T.-H. Shin and J. Cheon, *Acc. Chem. Res.*, 2011, **44**, 863-874.
173. M. Nahrendorf, E. Keliher, B. Marinelli, P. Waterman, P. F. Feruglio, L. Fexon, M. Pivovarov, F. K. Swirski, M. J. Pittet, C. Vinegoni and R. Weissleder, *Proc. Natl. Acad. Sci. USA*, 2010, **107**, 7910-7915.
174. D. W. Hwang, H. Y. Ko, S.-K. Kim, D. Kim, D. S. Lee and S. Kim, *Chem. Eur. J.*, 2009, **15**, 9387-9393.

175. G. Sun, J. Xu, A. Hagooly, R. Rossin, Z. Li, D. A. Moore, C. J. Hawker, M. J. Welch and K. L. Wooley, *Advanced Materials*, 2007, **19**, 3157-3162.
176. H. M. E. Azzazy and M. M. H. Mansour, *Clin. Chim. Acta*, 2009, **403**, 1-8.
177. M. Ritzi-Lehnert, *Expert. Rev. Mol. Diagn.*, 2012, **12**, 189-206.
178. M. Ritzi-Lehnert, R. Himmelreich, H. Attig, J. Claussen, R. Dahlke, G. Grosshauser, E. Holzer, M. Jeziorski, E. Schaeffer, A. Wende, S. Werner, J. O. Wiborg, I. Wick, K. S. Drese and T. Rothmann, *Biomed. Microdevices.*, 2011, **13**, 819-827.
179. C. Rehbock, V. Merk, L. Gamrad, R. Streubel and S. Barcikowski, *Phys. Chem. Chem. Phys.*, 2013, **15**, 3057-3067.
180. A. d. Giacomo, M. Dell'Aglio, A. Santagata, R. Gaudiuso, O. d. Pascale, P. Wagener, G. C. Messina, G. Compagnini and S. Barcikowski, *Phys. Chem. Chem. Phys.*, 2013, **15**, 3083-3092.
181. C. Sönnichsen, T. Franzl, T. Wilk, G. v. Plessen, J. Feldmann, O. Wilson and P. Mulvaney, *Phys. Rev. Lett.*, 2002, **88**, 077402.
182. C. Sönnichsen and A. P. Alivisatos, *Nano Lett.*, 2004, **5**, 301-304.
183. P. Rilling, T. Walter, R. Pommersheim and W. Vogt, *J. Membr. Sci.*, 1997, **129**, 283-287.
184. Y. Zhao, J. Fickert, K. Landfester and D. Crespy, *Small*, 2012, **8**, 2954-2958.
185. F. Goycoolea, A. Valle-Gallego, R. Stefani, B. Menchicchi, L. David, C. Rochas, M. Santander-Ortega and M. Alonso, *Colloid Polym. Sci.*, 2012, **290**, 1423-1434.
186. K. Pan, Q. Zhong and S. J. Baek, *J. Agric. Food Chem.*, 2013, **61**, 6036-6043.
187. G. Clergeaud, R. Genç, M. Ortiz and C. K. O'Sullivan, *Langmuir*, 2013, **29**, 15405-15413.
188. R. C. den Dulk, K. A. Schmidt, G. Sabatte, S. Liebana and M. W. J. Prins, *Lab. Chip.*, 2013, **13**, 106-118.
189. P. Nadal, A. Pinto, M. Svobodova, N. Canela and C. K. O'Sullivan, *PLoS ONE*, 2012, **7**, e35253 EP -.
190. T. Baier, S. Mohanty, K. Drese, F. Rampf, J. Kim and F. Schönfeld, *Microfluid. Nanofluidics.*, 2009, **7**, 205-216.
191. A. Ranzoni, G. Sabatte, L. J. van IJzendoorn and M. W. J. Prins, *ACS Nano*, 2012, **6**, 3134-3141.
192. O. Strohmeier, A. Emperle, G. Roth, D. Mark, R. Zengerle and F. v. Stetten, *Lab. Chip.*, 2013, **13**, 146-155.
193. B. Teste, F. Malloggi, J.-M. Siaugue, A. Varenne, F. Kanoufi and S. Descroix, *Lab. Chip.*, 2011, **11**, 4207-4213.
194. B. D. Chithrani and W. C. W. Chan, *Nano Lett.*, 2007, **7**, 1542-1550.
195. M. S. Ehrenberg, A. E. Friedman, J. N. Finkelstein, G. Oberdörster and J. L. McGrath, *Biomaterials*, 2009, **30**, 603-610.
196. W. Schartl, *Nanoscale*, 2010, **2**, 829-843.
197. S. Utech, C. Scherer and M. Maskos, *J. Magn. Magn. Mater.*, 2009, **321**, 1386-1388.
198. N. Sanvicens and M. P. Marco, *Trends Biotechnol.*, 2008, **26**, 425-433.
199. L. Richter, V. Charwat, C. Jungreuthmayer, F. Bellutti, H. Brueckl and P. Ertl, *Lab. Chip.*, 2011, **11**, 2551-2560.